551.521.61

The influence of the 15 μ carbon-dioxide band on the atmospheric infra-red cooling rate

By G. N. PLASS
*The Johns Hopkins University, Baltimore, U.S.A.**

(Manuscript received 12 October 1955, in revised form 23 March 1956)

SUMMARY

The upward and downward radiation flux and cooling rate are calculated for the 15 μ band of carbon dioxide. Results are obtained for three different carbon-dioxide concentrations from the surface of the earth to 75 km, and for six frequency intervals covering the band. The infra-red absorption measurements of Cloud (1952) are used for calculations, on a high-speed electronic computer, by a method which takes account of the pressure and Doppler broadening, the overlapping of the spectral lines, and the variation of the intensity and half-width of the spectral lines with temperature and pressure. The numerical integration is performed over intervals that are never larger than 1 km and average values over layers are not used. The cooling rate for the present atmospheric carbon-dioxide concentration is greater than 1°C/day from 24 km to 70 km and is greater than 4°C/day from 38 km to 55 km. The sum of the ozone and carbon-dioxide cooling rates is greater than 4°C/day from 33 km to 57 km and agrees reasonably well with the heating due to ozone absorption. The results for different carbon-dioxide concentrations indicate that the average temperature at the surface of the earth would rise by 3·6°C if the carbon-dioxide concentration were doubled and would fall by 3·8°C if the carbon-dioxide concentration were halved, on the assumption that nothing else changed to affect the radiation balance.

1. INTRODUCTION

The results of calculations of the infra-red radiation flux and the heating and cooling rates in the atmosphere for the spectral region from 12 μ to 18 μ are presented in this paper. The magnitude of the radiation flux in this region is determined largely by the properties of the 15 μ carbon-dioxide band. For atmospheric layers very close to the surface of the earth a correction must be introduced for absorption by water vapour. The radiation flux has been computed for three different carbon-dioxide concentrations when there are clear skies, and when clouds are present at one or the other of two different heights. All calculations were made from the surface of the earth to a height of 75 km. The assumed variation of temperature and pressure with height agrees closely with the values given by the Rocket Panel (1952).

The calculations are based on the carbon-dioxide absorption measurements of Cloud (1952). The radiation flux was obtained from these laboratory measurements by the same method as was used by Plass (1956a) for the spectral region near the 9·6 μ ozone band. Complete details of the method are given in that paper. However, for the carbon-dioxide calculations it was necessary to take into account the variation with temperature of the absorption in a given frequency interval; this was calculated from the partition function and the known dependence on temperature of the intensity and half-width of the spectral lines. The atmosphere is not divided into homogeneous layers for the purpose of this calculation, as this procedure may introduce large errors in the determination of the cooling rates. At each stage a careful estimate is made of the accuracy of the calculation.

An excellent survey of previous work on the carbon-dioxide absorption problem is given by Elsasser and King (1953). The pioneer work of Ladenburg and Reiche (1911) has been extended in recent years by Callendar (1941), Elsasser (1942), Kaplan (1950), and Yamamoto (1952). Kaplan (1952) and Elsasser and King (1953) have made the most extensive previous calculations of the absorption of the carbon-dioxide band.

* This paper was completed while the author was on leave of absence at Michigan State University. At present with Systems Research Corporation, Van Nuys, California.

2. Method for calculation of atmospheric transmission from laboratory data

The extensive and detailed study of the 15 μ carbon-dioxide band by Cloud (1952) was made on the large 100-foot absorption cell built by Professor John Strong at Johns Hopkins University. Path lengths up to 600 ft could be obtained by means of a six-fold optical path. The measurements were made with a wide slit so that the individual spectral lines were not resolved and the mean transmission could easily be obtained for various intervals. All the measurements made by Cloud are shown in Fig. 1 for the entire spectral interval from 12 μ to 18 μ. The logarithm of the fractional absorption, A, is plotted against the logarithm of the product of the pressure, p, and path length w, used in the laboratory. All the measured points lie on a single universal absorption curve within the experimental accuracy of about two per cent.

However, the entire interval from 12 μ to 18 μ must be divided into smaller intervals in order to calculate the radiation flux in the atmosphere. The black-body intensity is replaced by an average value over the interval in question in order to perform the integration over frequency. Since the black-body intensity varies with frequency very slowly compared with the extremely rapid variations of the absorption coefficient, it can be shown numerically that the substitution of an appropriate average value for the black-body intensity introduces no appreciable error for frequency intervals as large as one micron. For this reason the interval from 12 μ to 18 μ was divided into six intervals, each one micron wide, and all quantities were calculated for each of these intervals. The absorption measurements of Cloud (1952) for each of these intervals are shown in Figs. 2, 3 and 4.

The atmospheric radiation flux and cooling rate were calculated from these measured absorption curves by the method described by Plass (1952a). Details of the procedure, a discussion of the influence of the assumed temperature distribution on the final results, and detailed calculations of the probable error of the final results are described by Plass (1956a) for the similar calculations for ozone. In particular, the following corrections were made to the transmission function : (1) for Doppler broadening above 50 km (Plass and Fivel 1953); (2) extrapolation of experimental results to very small path lengths (Plass 1952a, 1954; Plass and Fivel 1955b); (3) multiplication of the path length by a numerical factor varying with the transmission, in order to obtain the diffuse radiation (Plass 1952b); (4) for the variation of line strength and half-width with temperature (the procedure for making this correction is given in the Appendix).

It was assumed that the mixing ratio for carbon dioxide is a constant independent of height up to 75 km. This is a good approximation for the average carbon-dioxide amount, except possibly very near the ground. The fluctuations of the carbon-dioxide mixing ratio are small compared to those of water vapour and ozone and should have very little influence on the radiation flux. The pressure and density curves given by the Rocket Panel (1952) were used with the necessary corrections for the small differences between their temperature and our assumed temperature.

The following temperature distribution was assumed for all the carbon-dioxide calculations :

$$
\begin{aligned}
T &= 288 - 6z & 0 &\leqslant z \leqslant 13 \text{ km} \\
T &= 210 & 13 &\leqslant z \leqslant 22 \text{ km} \\
T &= 210 + 3(z - 22) & 22 &\leqslant z \leqslant 43 \text{ km} \\
T &= 273 & 43 &\leqslant z \leqslant 54 \text{ km} \\
T &= 273 - 3(z - 54) & 54 &\leqslant z \leqslant 75 \text{ km},
\end{aligned}
$$

where z is the height in kilometres. These values agree closely with those given by the Rocket Panel (1952) and should represent an average temperature distribution in middle

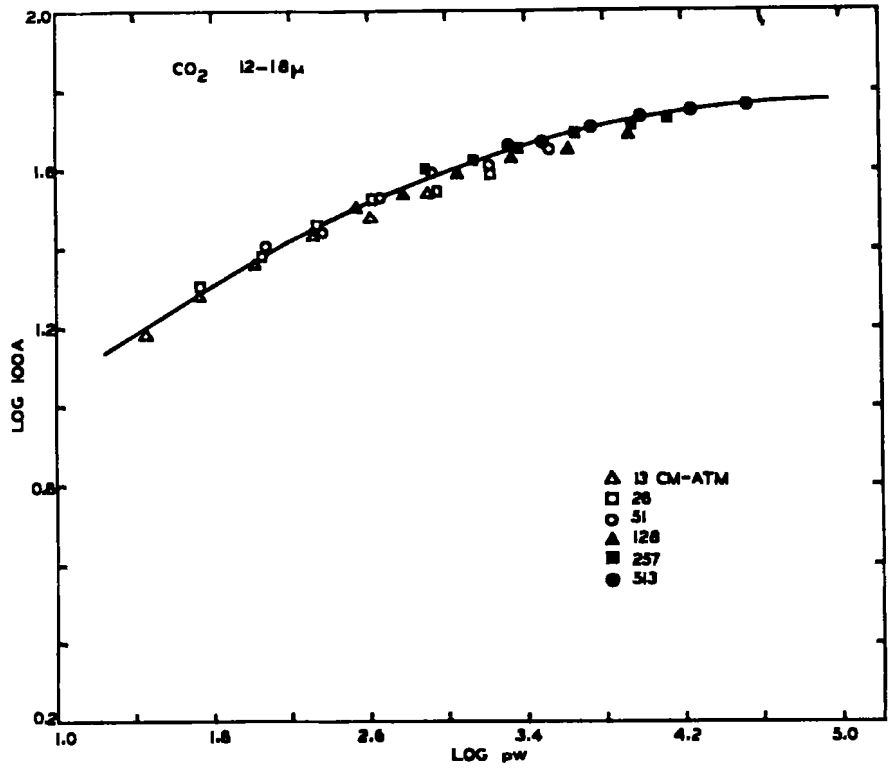

Figure 1. The fractional absorption, A, of CO_2 as a function of the product of the pressure, p, and the optical path length used in the laboratory, w, for the spectral interval from 12 μ-18 μ. The measurements were made by Cloud (1952).

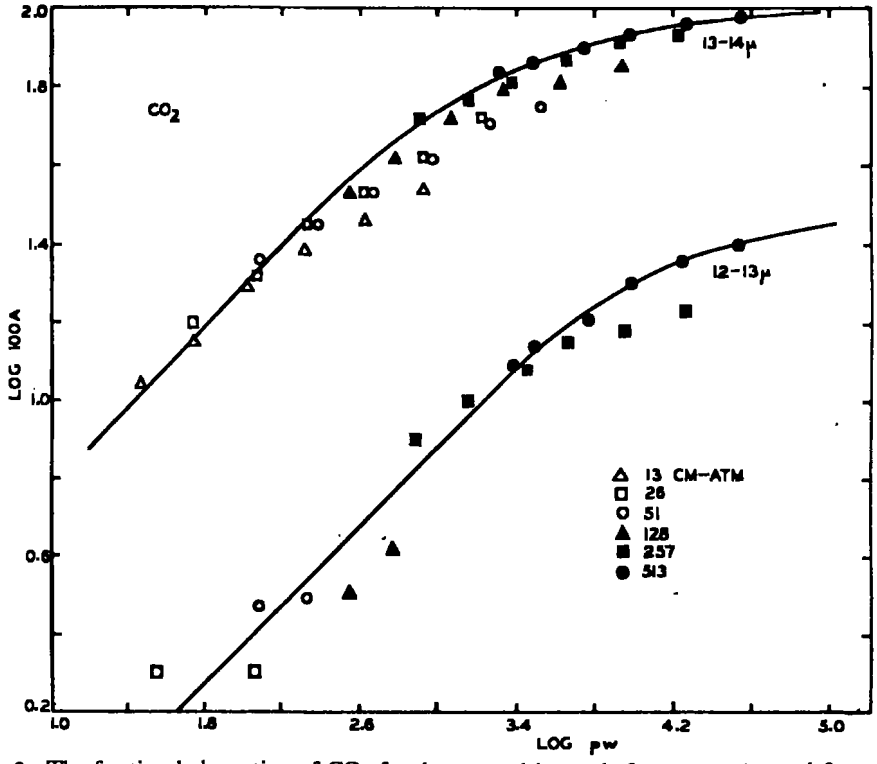

Figure 2. The fractional absorption of CO_2 for the spectral intervals from 12 μ-13 μ and from 13 μ-14 μ as measured by Cloud (1952).

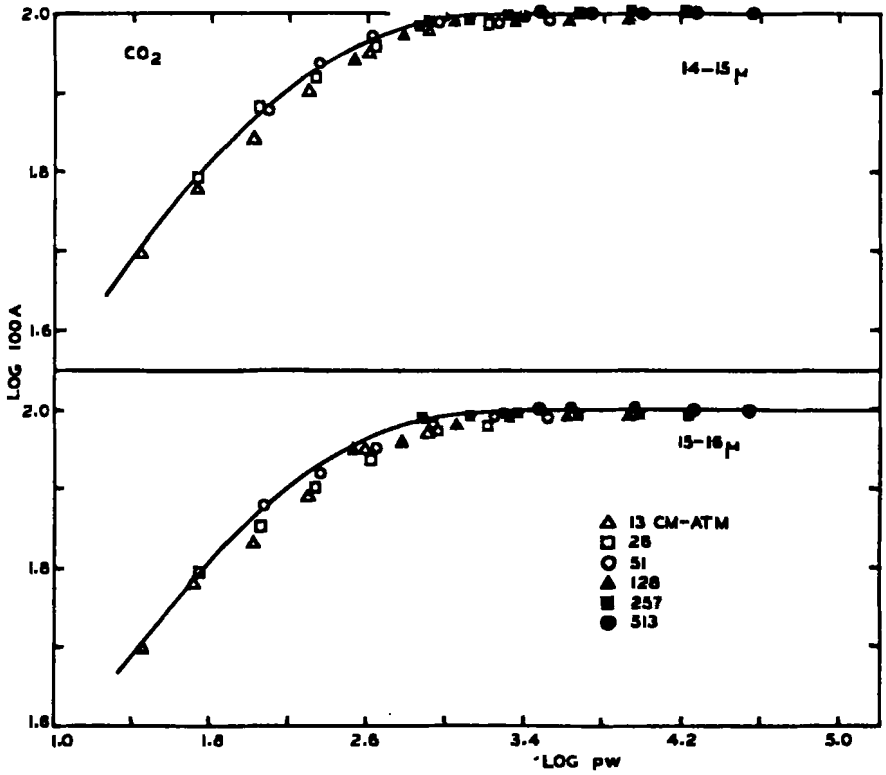

Figure 3. The fractional absorption of CO_2 for the spectral intervals from 14 μ-15 μ and from 15 μ-16 μ as measured by Cloud (1952).

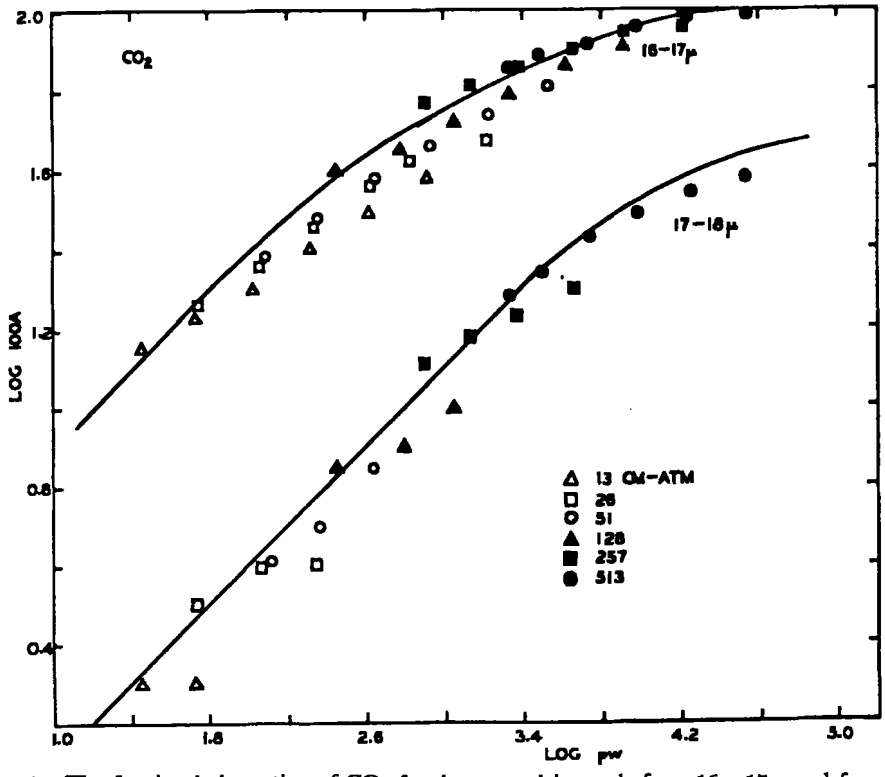

Figure 4. The fractional absorption of CO_2 for the spectral intervals from 16 μ-17 μ and from 17 μ-18 μ as measured by Cloud (1952).

latitudes. A more accurate result can be obtained from the same number of steps in the numerical calculation if the atmosphere can be divided into regions each of which has a linear variation of temperature with height, as here.

The necessary integrations over the transmission functions (Eqs. 1-3, Plass 1956a) were performed numerically for values of the integrand at intervals of 1 km. When the integrand was a rapidly varying function, even smaller intervals were chosen. The atmosphere was not divided into homogeneous layers for the purpose of this calculation, as this procedure may introduce large errors in the cooling rate. For each of the six spectral intervals, and for each of the three different carbon-dioxide concentrations, it was necessary to calculate the transmission function for approximately 3,000 pairs of values of z_0 and z_1 between the surface of the earth and 75 km, where z_0 and z_1 are the heights of the lower and upper level respectively. The entire numerical calculation, including the corrections to the transmission function, was coded for the MIDAC high-speed digital computer at the University of Michigan.

3. The infra-red radiation flux and cooling rate

The results of the calculation of the infra-red radiation flux and cooling rate by the above method are shown in Figs. 5-8. The upward and downward radiation flux is given for the entire spectral interval from 12 μ-18 μ and for three smaller intervals. In order to present as many of the results as possible in a reasonable space, the results for three pairs of intervals have been combined. Thus instead of showing the flux for the 12 μ-13 μ and 17 μ-18 μ intervals separately, as calculated, only the total for both intervals is given; the variation with height of the results for these two intervals is almost the same and no essential information is lost by combining the results in this manner. For the same reason the results for the 13 μ-14 μ and 16 μ-17 μ intervals were combined, as were those for the 14 μ-15 μ and 15 μ-16 μ intervals.

Figs. 5 and 6 give the results for the present concentration of CO_2 ($c = 5 \times 10^{-4}$; 0·033 per cent by volume) when the temperature correction in the Appendix is made (solid curve) and is not made (dashed curve).

The change in the upward flux with height depends on the transmission of the spectral region in question. If the transmission were unity in a given spectral interval, the higher atmospheric layers at lower temperatures would be unable to change the upward flux and it would be constant with height. If the transmission were zero, the upward flux would be equal to the black-body intensity at every height and, for our assumed temperature distribution, would have a minimum from 13 km to 22 km and maxima at the ground and from 43 km to 54 km.

The upward flux for various spectral intervals as shown in Fig. 5 is close to these limits. For the 12 μ-13 μ; 17 μ-18 μ interval the transmission is near unity; the upward flux is nearly constant with a value above 13 km only 8 per cent lower than the value at the ground. For the 13 μ-14 μ; 16 μ-17 μ interval the transmission has an intermediate value at the lower altitudes; between 13 km and 22 km the upward flux falls to almost one-half of its value at the ground. It increases slightly above 22 km, but this rise is very small, since the transmission is so near unity for paths at the higher altitudes that higher temperatures there can have little effect. For the 14 μ-16 μ interval the transmission is nearly zero up to 15 km; here the upward flux is very close to the black-body curve. Above this height the upward flux increases as the atmospheric temperature increases to a value 28 per cent above its minimum value. The upward flux for the entire range from 12 μ-18 μ exhibits the characteristics of a curve for a transmission function with a value intermediate between zero and unity.

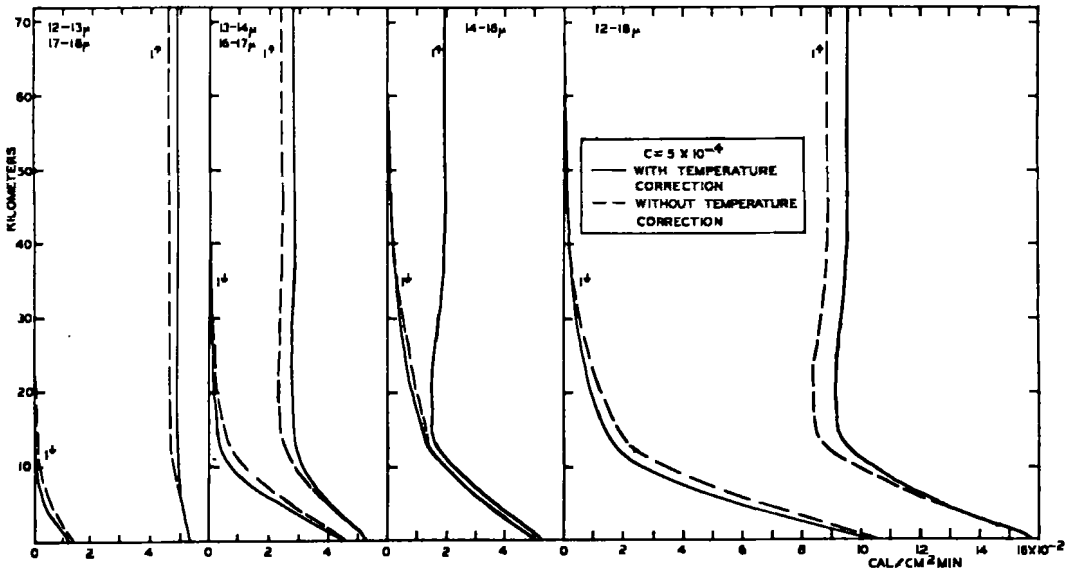

Figure 5. The upward and downward radiation flux as a function of height for the combined frequency intervals from 12 μ-13 μ and 17 μ-18 μ; from 13 μ-14 μ and 16 μ-17 μ; from 14 μ-16 μ; and for the entire interval from 12 μ-18 μ. The temperature correction described in the Appendix was made in the calculations for the solid curves and was omitted for the dashed curves. The present CO_2 concentration ($c = 5 \times 10^{-4}$; 0·033 per cent by volume) was assumed for this calculation. The difference between the two curves for the upward flux for the 14 μ-16 μ interval cannot be shown on the scale of this graph.

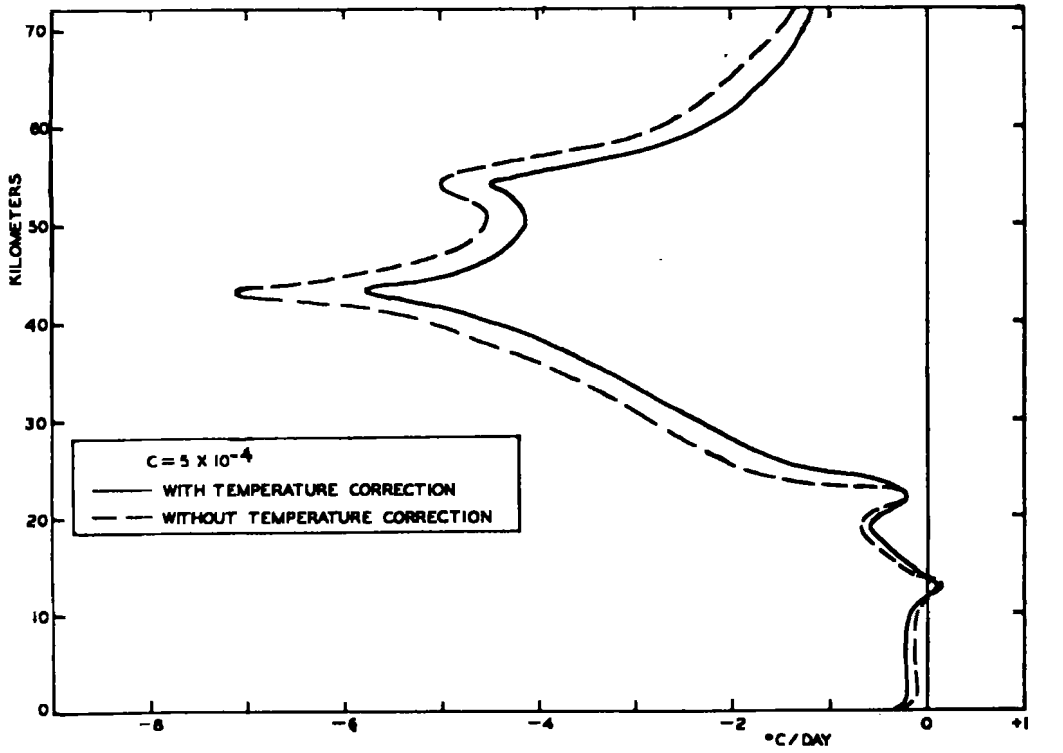

Figure 6. The cooling rate in °C/day for the entire frequency interval from 12 μ-18 μ.

There would be no downward flux if the transmission function were unity in a given frequency interval, since the atmosphere could not radiate at these frequencies. If the transmission function were zero, the downward flux would equal the black-body intensity for the appropriate temperature at a given height. For the interval from 12 μ-13 μ; 17 μ-18 μ the downward flux is quite small and has an appreciable value only below 10 km. For the interval from 13 μ-14 μ; 16 μ-17 μ the downward flux has a considerably larger value. For the interval from 14 μ-16 μ, the downward flux is larger than for either of the previous intervals and approaches the black-body flux below 13 km. The upward and downward flux would have an identical value equal to the black-body intensity below 13 km for the 14 μ-16 μ interval, if the transmission function were actually zero for all possible path lengths below 13 km. Actually for sufficiently small path lengths, even near the surface of the earth, the transmission function approaches unity; this is the reason for the small difference between the upward and downward flux in this case.

The cooling rate for the entire CO_2 band from 12 μ-18 μ is shown in Fig. 6. From the ground up to 10 km the cooling rate is of the order of a few tenths of a degree Celsius per day. This rate rises rapidly from 22 km to 43 km and reaches a maximum of 5·8°C per day at 43 km. The cooling rate is above 4·0°C per day from 38 km to 55 km. The rate decreases rapidly at higher altitudes. The maxima and minima in this curve at 13 km, 22 km, 43 km and 54 km arise from the discontinuities in the derivative of the assumed temperature curve at these altitudes (Plass 1956a). Such discontinuities seldom, if ever, actually exist in the atmosphere. Therefore the values in the neighbourhood of these maxima and minima should be smoothed out slightly when comparisons are made with the actual atmosphere. As discussed above, this temperature distribution was assumed, as it greatly increases the accuracy of numerical calculations carried to a given number of figures; it approximates closely the actual temperature distribution.

A comparison of the cooling rates of the ozone and carbon-dioxide bands is given Table 1. The ozone cooling rates are those calculated by Plass (1956a) for the ozone-concentration curve L and the temperature curve B as defined in that article. This temperature curve is very close to the one used for the present carbon-dioxide calculations, except that it does not have discontinuous derivatives at certain heights. A small correction has been made to the carbon-dioxide results between 40 km and 60 km to bring them more closely into agreement with the results that would have been obtained had the temperature curve B been used. The largest relative contribution from the ozone is at 45 km where it contributes 30 per cent to the total energy radiated from both ozone and carbon dioxide. The carbon dioxide is much more important than the ozone in cooling the atmosphere above 55 km.

TABLE 1. COOLING RATES IN THE STRATOSPHERE

Height (km)	Ozone (°C/day)	Carbon Dioxide (°C/day)	Total (°C/day)
25	0·1	1·3	1·4
30	0·5	2·4	2·9
35	1·3	3·3	4·6
40	1·8	4·5	6·3
45	2·1	4·9	7·0
50	1·5	4·6	6·1
55	0·8	4·0	4·8
60	0·3	2·3	2·6
65	0·1	1·7	1·8
70	0·0	1·3	1·3

The absorption of solar energy by ozone at these altitudes has recently been calculated by Johnson (1953) and Pressman (1955). Since the heating rates vary greatly with latitude and season (Pressman 1955), it is difficult to make quantitative comparisons. However, it is clear that the heating and cooling rates agree qualitatively and have their maxima at the same altitude (45 km) with approximately the same value of 7·0°C/day. The cooling due to H_2O is not included in Table 1. Differences between the heating and cooling rates could be ascribed to the possible additional cooling effect of H_2O and to uncertainties in the calculations themselves.

The correction for the variation of the line intensities and half-widths with temperature, discussed in the Appendix, greatly complicates the calculation and introduces an additional factor of uncertainty in the final results. In order to study the effect of this correction, the calculations were made with and without the temperature correction, for each of the three CO_2 concentrations. The results are shown in Figs. 5 and 6 for the present CO_2 concentration ($c = 5 \times 10^{-4}$). The principal temperature correction is due to the increase in line intensity of the stronger lines of the band with increasing temperature over the temperature range that occurs in the atmosphere. Since the laboratory measurements of the transmission function are made at room temperature, the temperature-corrected transmission function is greater than the uncorrected value for the colder regions of the atmosphere. Thus the results are changed most when the temperature correction is made at altitudes from 10 to 30 km where the atmospheric temperature is relatively low.

The value of the upward flux at high altitudes is 5 per cent higher for the interval from 12 μ-13 μ; 17 μ-18 μ, and 14 per cent higher for the interval from 13 μ-14 μ; 16 μ-17 μ, when the temperature correction is made than when it is not made. The upward flux has a larger value since the transmission function is closer to unity after the temperature correction. Thus the upward flux cannot follow so well the dip in the black-body curve in the lower stratosphere. The change for the 14 μ-16 μ interval cannot be shown on the scale of Fig. 5, since the transmission function is virtually zero in the lower part of the atmosphere in both cases.

For the downward flux the difference between the calculated values with and without the temperature correction is largest in each case near the base of the stratosphere. In the intervals from 12 μ-13 μ; 17 μ-18 μ, and from 13 μ-14 μ; 16 μ-17 μ, most of the downward radiation reaching, for example, 8 km, originates in the colder region of the atmosphere from 10 km to 30 km. It is not surprising therefore that the increased values for the transmission after the temperature correction is made give values for the downward flux that are as little as half those obtained without the correction. This is the only region of the atmosphere where the temperature correction must be made in order to obtain even approximately correct values of the flux. At the surface of the earth so much of the downward radiation comes from the lower, warmer layers of the atmosphere that the difference between the two curves is less than 10 per cent for the interval from 12 μ-13 μ; 17 μ-18 μ, and is very small for the other intervals.

The cooling curve with and without the temperature correction is given in Fig. 6. Above 14 km the cooling rates are slightly smaller when the temperature correction is made. However, the shapes of the two curves are remarkably similar and the percentage deviation of the two curves is not large except below 14 km where in any case the cooling rate due to CO_2 is not of great importance. Thus it would appear that reasonably accurate calculations of the cooling rate above 14 km can be made if desired without introducing the complexities of the temperature correction.

The infra-red flux and cooling rates are shown in Figs. 7 and 8 for three different CO_2 concentrations, 0·025, 0·05 and 0·10 per cent by weight or 0·0165, 0·033 and 0·066 per cent by volume. The lowest and highest values correspond to halving or doubling

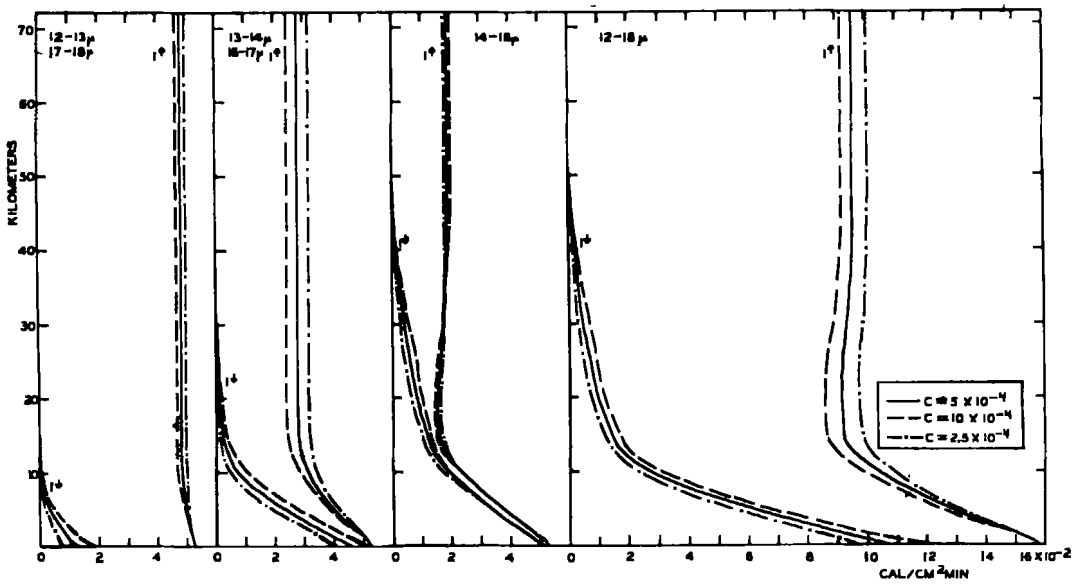

Figure 7. The upward and downward radiation flux as a function of height for the combined frequency intervals from 12 μ-13 μ and 17 μ-18 μ; from 13 μ-14 μ and 16 μ-17 μ; from 14 μ-16 μ; and for the entire interval from 12 μ-18 μ. Curves are given for the following CO_2 concentrations: $c = 5 \times 10^{-4}$ (0·033 per cent by volume); $c = 10 \times 10^{-4}$ (0·066 per cent by volume); $c = 2{\cdot}5 \times 10^{-4}$ (0·0165 per cent by volume). The temperature correction described in the Appendix was made in the calculation of all these curves.

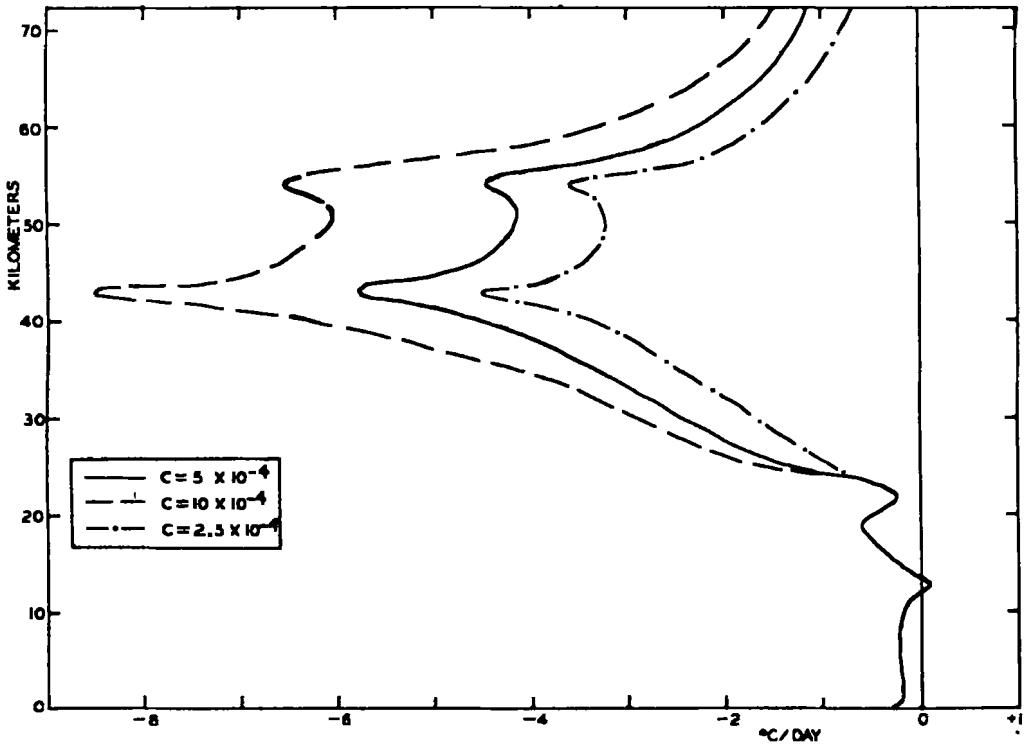

Figure 8. The cooling rate in °C/day for the entire frequency interval from 12 μ-18 μ. Curves are given for the following CO_2 concentrations : $c = 5 \times 10^{-4}$ (0·033 per cent by volume); $c = 10 \times 10^{-4}$ (0·066 per cent by volume); $c = 2{\cdot}5 \times 10^{-4}$ (0·0165 per cent by volume). The temperature correction described in the Appendix was made in the calculation of all these curves. There is no difference in the cooling rates below 24 km within the accuracy of the calculation and only one curve is shown in this region.

the present atmospheric CO_2 amount. The temperature correction has been made to all the results given in these figures, since the complete procedure had been coded for the MIDAC electronic computer.

For the intervals from 12 μ-13 μ; 17 μ-18 μ, and from 13 μ-14 μ; 16 μ-17 μ, the upward flux is smaller the larger the CO_2 concentration, since the smaller transmission function allows the flux to approach closer to the black-body flux at the temperature minimum from 13 km to 22 km. The same is true for the interval from 14 μ-16 μ below 32 km. Above this height the upward flux is slightly greater for larger CO_2 concentrations, since the transmission function is still sufficiently small in this region for the upward radiation to increase slightly owing to the higher temperature in the upper part of the stratosphere. Similar remarks apply to the downward flux. In this case the larger CO_2 concentrations give the larger values for the downward flux.

The cooling rates are given in Fig. 8 for these three different CO_2 concentrations. There was no definite difference within the accuracy of the calculation, in the cooling rates below 24 km, and only one curve is shown in this region. At higher altitudes the cooling rate increases appreciably if the CO_2 concentration changes. At the maximum of the cooling curve at 43 km, the cooling rate increases from 5·8°C/day to 8·5°C/day if the CO_2 concentration is doubled.

Numerous checks were made during the progress of these calculations in order to determine the accuracy of the final results. The procedure was similar to the one used by Plass (1956a) for ozone. The upward and downward flux is determined with a percentage error smaller than that of the original laboratory absorption measurements. Cloud's estimate of a 2 per cent error in the laboratory measurements of the transmission function may be somewhat optimistic. A conservative estimate of the error in the upward and downward flux, taking into account the various corrections made in the course of the calculations, is 3 per cent. However, the relative changes of the curves for different concentrations are determined with considerably greater accuracy than this. The probable error of the cooling rate is estimated by introducing arbitrary variations into the original transmission functions and calculating their influence on the final result. The probable error obtained in this manner is about 10 per cent below 20 km, increasing to 30 per cent at 50 km and becoming rather uncertain above 60 km. Again the relative differences between the various curves should be considerably more accurate than their magnitude.

4. Temperature variations at the surface of the earth

The change in the equilibrium temperature at the surface of the earth with CO_2 concentration can be estimated from the corresponding variations of the radiation flux, if it is assumed that nothing else changes to alter the radiation balance when the CO_2 amount varies. In order to obtain the temperature change it is also assumed that an additional amount of radiant energy equal to 0·0033 Cal cm^{-2} min^{-1} would be radiated to space, if the average temperature of the earth's surface were to increase by 1°C. This number cannot be calculated accurately until a detailed study has been made of the H_2O spectrum, but it represents the best value that can be given with our present knowledge of this spectrum. When a more accurate value for this number is obtained in the future, all the temperature changes given here should be multiplied by the ratio of the old to the new value.

When the CO_2 amount is doubled and halved the change in the downward flux at the surface of the earth is 0·0119 and 0·0125 Cal cm^{-2} sec^{-1} respectively. Thus, in order to restore equilibrium the surface temperature must rise by 3·6°C if the CO_2 concentration is doubled and the surface temperature must fall by 3·8°C if the CO_2

concentration is halved. It is interesting to note that the four intervals from 12 μ-13 μ, 13 μ-14 μ, 16 μ-17 μ and 17 μ-18 μ contribute about equally to this temperature change. The interval from 14 μ-16 μ does not contribute since it is opaque near the ground at all these concentrations. The argument has sometimes been advanced that the CO_2 cannot cause a temperature change at the surface of the earth because the CO_2 band is always black at any reasonable concentration. This argument is true for the lines near the centre of the band from 14 μ-16 μ, but neglects completely the important contribution of the lines farther from the band centre.

This same method shows that the average temperature is lowered 2·2°C and 1·3°C at the upper surface of a cloud at 4 km and 9 km respectively, if the amount of CO_2 in the atmosphere is halved. This temperature change at the upper surface of a cloud could be the cause of the increased precipitation at the beginning of a glacial period (Plass 1956b).

If the CO_2 concentration is doubled, Arrhenius (1896) calculated a temperature increase of 6°C, Hulbert (1931) of 4°C, and Callendar (1938) of 2°C. The value of 3·6°C obtained from the present study is based on more accurate experimental data than were available previously and it was possible to perform the elaborate calculations only because an electronic computer was available. Such factors as the weak lines that are relatively far from the band centre and the change in intensity and half-width of the spectral lines with temperature and pressure were taken into account in the present calculations.

The radiation calculations predict a definite temperature change for every variation in CO_2 amount in the atmosphere. These temperature changes are sufficiently large to have an appreciable influence on the climate. Plass (1956b) has considered the various factors that control the CO_2 content of the atmosphere and oceans and has discussed the current status of the carbon dioxide theory of climatic change.

Acknowledgments

This research was supported by the Office of Naval Research, Washington. I wish to thank Mr. L. Leopold for his extensive and careful work in calculating the radiative flux in the early stages of this study. His work made it possible to code the final calculation for the MIDAC high-speed electronic computer.

Appendix

Variation of transmission function with temperature

Laboratory measurements of the absorption of atmospheric gases should ideally be made over the range of temperatures that occur in the atmosphere. This would eliminate the need to make a theoretical estimate of the variation of the transmission function with temperature. However, to our knowledge no suitable measurements have yet been made at temperatures below room temperature.

First let us assume that the temperature decreases linearly with height between z_0 and z_1. Without any loss of generality z_0 may be set equal to zero. Then the temperature dependence is given by

$$T = T_0 - a z \quad . \quad . \quad . \quad . \quad (1)$$

and the pressure dependence by

$$p = p_0 (T/T_0)^{Mg/aR} \quad . \quad . \quad . \quad . \quad (2)$$

The temperature dependence of the line intensity, S, and, to a smaller extent, the temperature variation of the half-width of the spectral line, α, cause the transmission function to vary with temperature. The theoretical variation with temperature of both these factors is known. From the Maxwell-Boltzmann distribution law and the rotational partition function, it follows that the temperature dependence of S is given by the expression

$$\frac{S(T)}{S(T_0)} = \frac{T_0}{T} \exp\left[-\frac{E_J}{kT} + \frac{E_J}{kT_0}\right] \quad . \quad . \quad . \quad (3)$$

where T_0 is a standard temperature, $S(T)$ and $S(T_0)$ are the line intensities at the temperatures T and T_0 respectively, E_J is the energy of the initial state of the transition, and k is the Boltzmann constant. Other terms in the general expression for S which change very slowly with T are omitted from Eq. (3), since numerical integration shows that their effect is very small for the range of temperatures in the atmosphere.

From kinetic theory it follows that

$$\alpha = \alpha_0 (p/p_0) (T_0/T)^{\frac{1}{2}} \quad . \quad . \quad . \quad . \quad (4)$$

where α_0 is the half-width at a standard pressure and temperature, p_0 and T_0. Although the dependence of α on pressure has been verified, a square-root temperature dependence should not be expected for all lines. However, the variation of α with temperature introduces only a very small correction.

For a single spectral line, the result of the usual method for the calculation of the absorption in the atmosphere integrated over frequency, A, (Plass 1954, Plass and Fivel 1955a) is that

$$A(u_0, u_1) = \left\{4 \sec\theta \int_{u_0}^{u_1} S\,\alpha\, du\right\}^{\frac{1}{2}} \quad . \quad . \quad . \quad (5)$$

for the strong-line approximation and that

$$A(u_0, u_1) = \sec\theta \int_{u_0}^{u_1} S\, du \quad . \quad . \quad . \quad . \quad (6)$$

for the weak-line approximation, where

$$u = \int_z^\infty c\,\rho\, dz,$$

$$A(u_0, u_1) = \int_0^\infty [1 - \tau(u_0, u_1)]\, d\nu,$$

θ is the angle the radiation makes with the vertical, c is the ratio of the density of the radiating gas to the total density, ρ, and τ is the transmission function. Eqs. (5) and (6) are valid regardless of the functional dependence of S on height. The results for overlapping spectral lines are discussed later in this section.

In order to obtain the integrated absorption, A, for the strong-line approximation, substitute Eqs. (1), (2), (3) and (4) into Eq. (5). Define an effective temperature, T_e, between z_0 and z_1 so that the integrated absorption, $A(z_0, z_1)$, for a radiating gas in a hypothetical atmosphere with the same temperature, T_e, at all heights, is the same as for the actual radiating gas with variable temperature. The effective temperature, T_e, is a function of both z_0 and z_1. It can be calculated by setting the expression for A, obtained

from Eq. (5) when the entire atmospheric layer is at the temperature T_e, equal to the expression for A, derived above, which is valid when the temperature decreases linearly with height.

In this manner it is found that T_e can be determined from the other known constants of the problem, from the equation

$$\int_1^{\beta} \exp\left(-\frac{E_J y}{kT_0}\right) y^{-\frac{2Mg}{aR}+\frac{1}{2}}\, dy = \left(\frac{T_0}{T_e}\right)^{\frac{3}{2}} \frac{aR}{2Mg}\left[1-\beta^{-\frac{2Mg}{aR}}\right] \exp\left(-\frac{E_J}{kT_e}\right). \quad (7)$$

where $$\beta^{-1} = 1 - (az_1/T_0).$$

The value of the effective temperature, T_e, can be obtained as a function of z_0 and z_1 from the numerical solution of Eq. (7). Some typical results are shown in Fig. 9, where T_e is plotted against the temperature at the boundary of the layer. The upper set of three curves gives T_e for a layer between z_0, where the temperature is 293°K, and z_1, where the temperature has the value given by the abscissa. The lower set of three curves gives T_e for a layer extending from z_0, where the temperature has the value given by the abscissa, to z_1, where the temperature is 218°K. Each set of curves is drawn for three different values of the ratio $m = E_J/kT_{293}$. Since the value of m does not change by more than a factor of three when averaged over a frequency interval of 0·1 μ or more in the range from 12 μ-18 μ, Fig. 9 shows that the value of T_e is insensitive to the assumed value of m.

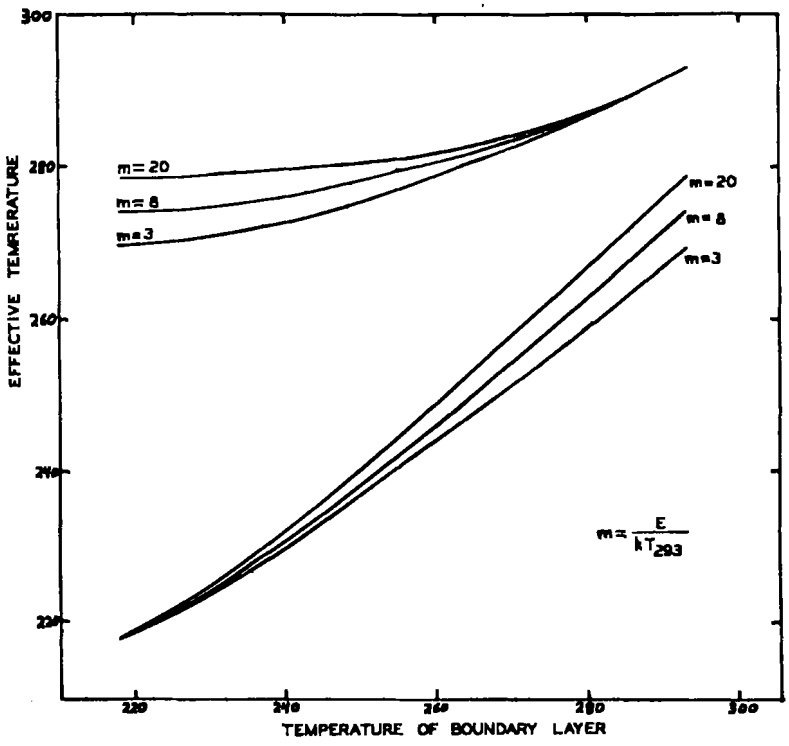

Figure 9. The upper set of three curves gives the value of the effective temperature, T_e, for an atmospheric layer extending from a fixed height where the temperature is 293°K to a height where the temperature has the value given by the abscissa. The lower set of three curves gives the value of T_e for an atmospheric layer extending from a height where the temperature has the value given by the abscissa to a fixed height where the temperature is 218°K. Each set of curves is drawn for three different values of the ratio $m = E_J/kT_{293}$, where E_J is the energy of the initial state of the transition.

When the equation for the weak-line approximation, Eq. (6), is used instead of Eq. (5), a similar derivation to the one given above shows that

$$\int_1^{\beta} \exp\left(-\frac{E_J y}{kT_0}\right) y^{-\frac{Mg}{aR}-1}\, dy = \left(\frac{T_0}{T_e}\right)\frac{aR}{Mg}\left[1-\beta^{-\frac{Mg}{aR}}\right]\exp\left(-\frac{E_J}{kT_e}\right) \quad . \quad . \quad (8)$$

The results for T_e are very similar to those obtained from Eq. (7).

Eqs. (7) and (8) have been derived for a single spectral line. However, the identical equations are also valid for the Elsasser model of a band in the limits of the strong- and weak-line approximations. This result can be derived from the equations for the Elsasser model given by Plass and Fivel (1955b). Since T_e does not depend on the degree of overlapping of the spectral lines for the Elsasser model in the limits of the strong- and weak-line approximations, it appears that T_e cannot vary appreciably with the degree of overlapping of the spectral lines for any model of a band.

Equations similar to Eqs. (7) and (8) were derived for the cases when the temperature increases linearly with height or when there are several regions with a constant temperature in one region and a linear increase or decrease in another. In practice, for the temperature distribution assumed for this calculation, it is never necessary to use more than two regions with different lapse rates for the calculation of T_e. If more than two regions exist with different lapse rates between z_0 and z_1, the regions above the first two make a negligible contribution.

The values of the ratio E_J/kT, where T is the temperature at which the laboratory absorption measurements were made, were calculated from a tabulation of the carbon dioxide lines kindly made available to us by Dr. L. D. Kaplan in advance of publication. The region from 12 μ to 18 μ was divided into intervals 0·1 μ wide. In each of these 60 intervals the average energy of the lines was computed. It was weighted either with the square-root of the line intensity or the first power of the intensity depending on whether the absorption for the entire interval followed the strong-line or the weak-line approximation respectively for the path length between z_0 and z_1. The average energy for the six intervals of one micron width from 12 μ to 18 μ was then calculated from the averages for the 0·1 μ intervals. The deviations of the values for the 0·1 μ intervals from the average for the 1 μ intervals were relatively small. For example, for the interval from 12 μ to 13 μ the average deviation of the results for the smaller intervals was only 10 per cent of the average value for the entire interval.

The calculated value of E_J/kT was between 3 and 8 for each of the six intervals of 1 μ width. Fig. 9 shows that T_e is insensitive to the value of E_J/kT. Thus it is possible to obtain the value of T_e for any combination of values of z_0 and z_1 with an estimated probable error of no more than a few degrees Kelvin.

Curves similar to those in Fig. 9 were plotted at intervals of 1 km from the surface of the earth to 75 km. They were calculated from Eqs. (7) and (8) or, when the temperature did not decrease linearly with height, from equivalent equations. The effective temperature, T_e, was determined in this manner for each pair of values of z_0 and z_1. The temperature correction to the integrated absorption was then calculated from Eqs. (3), (4) and the known equations for the dependence of the absorption on these variables (Plass 1952a, 1954; Plass and Fivel 1955b). Fortunately it was possible to code a programme of calculations for the MIDAC high-speed digital computer to calculate this correction entirely automatically for each pair of z_0 and z_1.

All the carbon-dioxide calculations were made both with and without this temperature correction. The correction was largest for the intervals, from 12 μ-13 μ and 17 μ-18 μ, that are far from the centre of the band, and was smallest for the region from 14 μ-16 μ at the centre of the band.

References

Arrhenius, S.	1896	*Phil. Mag.*, **41**, p. 237.
Callendar, G. S.	1938	*Quart. J. R. Met. Soc.*, **64**, p. 223.
	1941	*Ibid.*, **67**, p. 263.
Cloud, W. H.	1952	'The 15 μ band of CO_2 broadened by nitrogen and helium,' Johns Hopkins Univ.
Elsasser, W. M.	1942	'Heat transfer by infra-red radiation in the atmosphere,' *Harvard Met. Studies*, No. 6.
Elsasser, W. M. and King, J. I.	1953	'Stratospheric radiation,' *Tech. Rep. Univ. Utah*, No. 9.
Hulbert, E. O.	1931	*Phys. Rev.*, **38**, p. 1876.
Johnson, F. S.	1953	*Bull. Amer. Met. Soc.*, **34**, p. 106.
Kaplan, L. D.	1950	*J. Chem. Phys.*, **18**, p. 186.
	1952	*J. Met.*, **9**, p. 1.
Ladenburg, R. and Reiche, F.	1911	*Ann. Phys.*, **42**, p. 181.
Plass, G. N.	1952a	*J. Opt. Soc. Amer.*, **42**, p. 677.
	1952b	*J. Met.*, **9**, p. 429.
	1954	*Ibid.*, **11**, p. 163.
	1956a	*Quart. J. R. Met. Soc.*, **82**, p. 30.
	1956b	*Tellus*, **8** (in press).
Plass, G. N. and Fivel, D. I.	1953	*Astrophys. J.*, **117**, p. 225.
	1955a	*Quart. J. R. Met. Soc.*, **81**, p. 48.
	1955b	*J. Met.*, **12**, p. 191.
Pressman, J.	1955	*Ibid.*, **12**, p. 87.
Rocket Panel	1952	*Phys. Rev.*, **88**, p. 1027.
Yamamoto, G.	1952	*Sci. Rep. Tohoku Univ.*, Ser. 5, Geophys., **4**, p. 9.